

Effect of sandblasting on the characterization of 95MXC coating layer on 304 stainless steel prepared by the TWAS (twin wire arc spray) coating method

Deni Fajar Fitriyana^{1*}, Windy Desti Puspitasari¹, Agustinus Purna Irawan², Januar Parlaungan Siregar³, Tezara Cionita⁴, Natalino Fonseca Da Silva Guterres⁵, Mateus De Sousa Da Silva⁵, Jamiluddin Jaafar⁶

¹ Department of Mechanical Engineering, Universitas Negeri Semarang, Semarang 50229, Indonesia

² Faculty of Engineering, Universitas Tarumanagara, Jakarta 11480, Indonesia

³ Faculty of Mechanical & Automotive Engineering Technology, Universiti Malaysia Pahang, 26600 Pekan, Malaysia

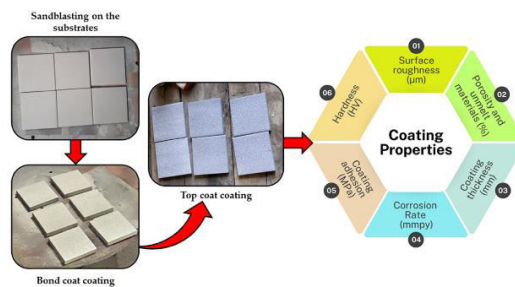
⁴ Faculty of Engineering and Quantity Surveying, INTI International University, Nilai 71800, Malaysia

⁵ Departement of Mechanical Engineering, Dili Institute of Technology, Timor Leste

⁶ Faculty of Mechanical and Manufacturing Engineering, Universiti Tun Hussein Onn Malaysia, Batu Pahat 86400, Johor, Malaysia

✉ deniifa89@mail.unnes.ac.id

This article contributes to:



Highlights:

- Sandblasting significantly increases the surface roughness of the 304 stainless steel substrates.
- The substrate's surface roughness has a significant impact on the quality of coating layers prepared by the TWAS method.
- The best specimen in this study is specimen A, with a percentage of unmelted material and porosity, thickness, hardness, and adhesion of 7.122%, 0.125 mm, 1081.6 HV, and 14.5 MPa, respectively.

Abstract

Twin wire arc spraying (TWAS) is a thermal spray process that is widely used in various industries. Nevertheless, the impact of repeated sandblasting on the coating characteristics of FeCrBSiMn coating created using the TWAS technique has not been extensively researched. Therefore, this study aims to investigate the influence of repeated sandblasting on the properties of the FeCrBSiMn coating layer created using the TWAS process. The study used stainless steel 304, 75B, and FeCrBSiMn as the substrate, bond coat, and top coat materials. The substrate materials underwent sandblasting with a repetition of 1, 2, and 3 cycles before the coating procedure. The coating's quality in this study was assessed using surface roughness, thickness, hardness, corrosion rate, bond strength, and Scanning Electron Microscope (SEM) examination. The findings of this investigation indicate that the sandblasting treatment substantially elevates the surface roughness of 304 stainless steel substrates. As the substrate surface becomes rougher, there is an increase in the percentage of porosity and unmelted material, as well as an increase in the thickness of the coating layer. Furthermore, the hardness of the resulting coating layer diminishes. Specimen A exhibited superior qualities in comparison to the other specimens. The coating layer on this specimen has a percentage of unmelted material and porosity, thickness, hardness and adhesion of 7.122%, 0.125 mm, 1081.6 HV and 14.5 MPa respectively. This investigation's results indicate that the substrate material's corrosion rate ($\times 10^{-6}$ mmpy) is 3648.6, which is lower than the corrosion rate of specimen A, which is 37.802.

Keywords: Impeller; Twin Wire Arc Spray (TWAS); Sandblasting; Stainless steel; 95MXC

Article info

Submitted:
2024-01-24

Revised:
2024-07-31

Accepted:
2024-11-07



This work is licensed under a Creative Commons Attribution-NonCommercial 4.0 International License

Publisher

Universitas Muhammadiyah
Magelang

1. Introduction

A pump is a device that utilizes mechanical energy to enhance the static pressure of a fluid, allowing a quick transfer of fluid from one place to another [1]–[4]. Pumps are used in various areas of human being, such as surface water purification and distribution, treatment of wastewater, oil and chemical businesses, and home water supply [5]. The impeller is one of the main components of the pump that continues to rotate to convert mechanical energy into velocity energy in liquid fluid [6]. This impeller often fails, such as wear that occurs due to several factors such as erosion, corrosion, and cavitation. Erosion is caused by the impact of solid or liquid particles on the impeller surface. Corrosion is caused by chemical and electrochemical reactions. Cavitation that occurs due to vapor bubbles and bursts, causing holes in the impeller [7].

Pumps are frequently employed during work to convey dirty liquids that have a high concentration of solid particles. The elevated concentration of particulate matter in the fluid flow can lead to erosion and corrosion of the impeller in the pump [8]. The impeller blade wear may be caused by hydro-abrasive erosion. Hydro-abrasive erosion on the pump impeller blade is caused by the presence of solid particles in water and is impacted by various factors, such as [9]:

- The properties of solid particles, including their size, form, concentration, and mineral composition.
- The flow characteristics include temperature, angle of impingement, flow velocity, operating time, and medium effect.
- The material characteristics of the substrate or pump impeller, including surface characteristics, coating qualities, and hardness.

Typically, solid particles in the liquid being pumped can lead to substantial erosion in the flow pathway, resulting in reduced efficiency and lifespan of the pump, ultimately causing significant output losses. Furthermore, extended exposure to friction can lead to the fracture of impeller blades, subsequently resulting in more extensive damage [10]. The interaction among fluid, particles, and impeller gives rise to complex flow patterns within the impeller channels. The impeller discharges solid particles at a high velocity, resulting in forceful collisions with the pump casing. This leads to energy dissipation and a significant likelihood of wear on other pump parts [11].

Coating is the process of applying a thin layer of material on the surface of a substrate to achieve desired biocompatibility, mechanical, tribological, protective, or decorative characteristics [12]–[21]. Coatings are commonly applied to pump impellers to enhance their resistance to wear, corrosion, erosion, and overall lifetime [22]–[27]. Utilizing sacrificial wear layers composed of metal coatings is an effective method for preventing wear on the impeller surface. Coatings can be applied to the impeller to decrease the duration and expenses of repairs and enhance its lifespan. Twin-wire arc spraying (TWAS) has been investigated for applying coatings of Fe, Ni, or carbide composite alloys onto the surface of the substrate without damaging the substrate surface [28]. In addition, The TWAS technique has effectively applied steels, aluminum, aluminum alloys, nickel alloys, and Inconel coatings into a comparable group of base metals [29]. TWAS is a thermal spray process that is a popular choice for remanufacturing due to its ability to deposit a diverse selection of surface coating materials at high deposition rates and a reasonable cost. TWAS uses two wires inserted into the injection machine, and an electric arc is ignited between the two ends of the wire so that when the wire melts quickly, the melt is shot by compressed gas and hardens on the surface being coated [30], [31]. This coating method has the advantages of low operating costs, high spray rate and more efficient coating deposition so as to improve mechanical properties and corrosion resistance [31]–[33]. In general, the TWAS technology can generate extremely dense metal coatings used in various applications to enhance durability against erosion, heat, corrosion, and wear. These applications are particularly relevant in power generation, medical industries, automotive, and aerospace [33].

The qualities of the coating layer formed by the TWAS process are influenced by various factors, such as post heat treatment, arc voltage, arc current, stand-off distance, traversal speed, and atomization gas pressure [5], [29], [34]–[36]. However, the influence of sandblasting on the properties of the coating layer generated by the TWAS method has not been extensively investigated. Sandblasting is a method of surface preparation used to clean and enhance the roughness on the surface of the substrate. This is done to facilitate strong adhesion of the coating layer [37]–[39]. Therefore, this study aims to investigate the influence of sandblasting on the characteristics of the coating layer produced by the TWAS technique. The substrate material used for the impeller in this study is 304 stainless steels. It will be coated using 75B as a bond coat and

95MXC as a top coat. Studying the impact of sandblasting on the analysis of the coating layer by the TWAS method has significant potential to enhance quality, production efficiency, and the advancement of new technologies for pump impeller manufacturing. A more durable and reliable pump impeller can be produced by understanding the interaction mechanism between the sandblasting process and the formation of the coating layer.

2. Material and Method

The substrate material utilized in this study is 304 stainless steel purchased from Tira Austenite Ltd., located in Semarang, Indonesia. The dimensions of the stainless steel substrate are 1000 mm in length, 100 mm in width, and 10 mm in thickness. The substrate material's density, comprehensive strength, elastic modulus, thermal expansion, and thermal conductivity are 8,000 Kg/m³, 210 MPa, 193 GPa, $17.2 \times 10^{-6}/K$, and 16.2 W/m.K, respectively [40]. Furthermore, in the coating process, TAFA 75B (NiAl) wire product was used as bond coat and TAFA 95MXC (FeCrBSiMn) wire product as top coat. The 75B and 95MXC wires utilized in this investigation were acquired from PT Cipta Agung in Surabaya, Indonesia. **Table 1** details the chemical composition comparison of the substrate, bond coat, and top coat materials. The properties of 75B and 95MXC are compared in **Table 2**.

Table 1.
Chemical composition comparison of the substrate, bond coat, and top coat materials

Elements	Substrate materials [36]	75B [41]	95MXC [42]
Al	–	5	–
Ni	8	95	–
Si	1	–	1.6
Cr	18	–	29
Mn	2	–	1.65
B	–	–	3.75
P	0.045	–	–
S	0.3	–	–
C	0.08	–	–
Fe	Balance	–	Balance

Table 2.
The properties of 75B and 95MXC

Parameters	75B [41]	95MXC [42]
Wire Size	1/16 in (1.6 mm)	1/16 in (1.6 mm)
Deposit Efficiency	70%	70%
Melting Point	2642°F (1450°C)	2200°F (1204°C) (approx.)
Bond Strength Tensile	9,100 psi clean surface (62.8 MPa) 9,750 psi blasted surface (67.2 MPa)	5775 psi @ 20 mils thick
Hardness	55-80 Rb (HRB)	As sprayed: 595 DPH (HV) After abrasive load: 1180 DPH (HV)
Coating Density	7.8 gm/cc	6.75 gm/cc

Figure 1 displays the experimental setup utilized in the current study. The substrate material was cut off using Everising S-12H cutting equipment provided by Bhinneka Bajasnas Ltd., in Semarang, Indonesia. This procedure aimed to create substrates with dimensions of 100 mm in length, 100 mm in breadth, and 10 mm in height. The surface roughness of substrates with predetermined dimensions was measured using an Elcometer 123 Surface Profile Gauge obtained from INDOMULTIMETER, Banten, Indonesia. The process of measuring surface roughness is based on the ISO 8503 standard. The study utilizes Garnet sand with a particle size of 40-60 mesh as the abrasive material in the sandblasting procedure. The sandblasting procedure was conducted via a Norblast Sandblasting machine, the NOB35CE model, manufactured by Norexco SA, located in Ville-la Grande, France. The sandblasting method involves using a pressure of 8 bar and a stand-off distance of 150 mm for 3 minutes. The sandblasting process was conducted using 1, 2, and 3 times in this investigation.

Table 3 displays the specimen codes and several sandblasting repetitions. The process for assessing surface roughness on the sandblasted substrate is the same as the procedure for measuring surface roughness on the substrate before sandblasting. The surface roughness was measured both before and after sandblasting, with the process being repeated three times. The average value was then determined based on these measurements. Before applying the coating, the substrate underwent a preheat treatment at a temperature of 100 °C. The coating was applied using a Miller Delta Weld 602 machine (Miller Electric, USA), with a 75B wire used as the bond coat and a 95MXC wire used as the top coat. The Miller Delta Weld 602 machine was

configured with a current of 200 A, voltage of 30 V, primary gas pressure of 3 bar, and a stand-off distance of 100 mm for the coating process of bond coat and top coat materials.

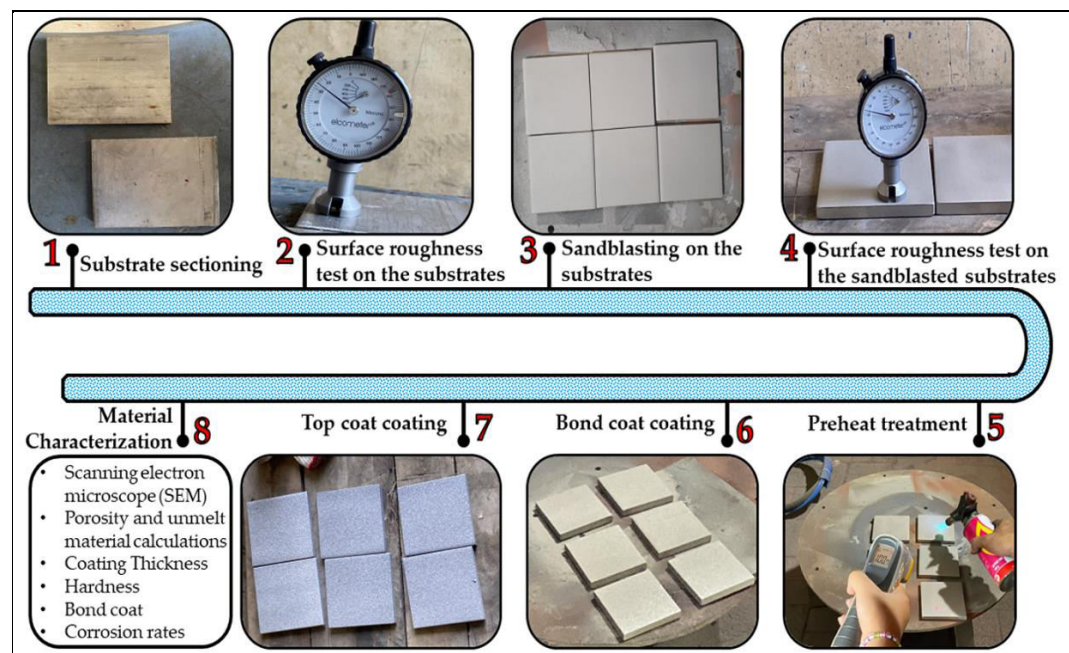


Figure 1. Experimental setup

Table 3. Specimens code

Specimens Code	Sandblasting Repetition (times)
RAW	-
A	1
B	2
C	3

Several tests were conducted to ascertain the sandblasting process's influence on the coated material's characterization, such as surface roughness, coating thickness, hardness, adhesion, corrosion rate, and Scanning Electron Microscope (SEM) testing. The surface roughness of substrates with predetermined dimensions was measured using an Elcometer 123 Surface Profile Gauge obtained from INDOMULTIMETER, Banten, Indonesia. The process of measuring surface roughness is based on the ISO 8503 standard. The test was conducted by positioning the instrument at multiple locations on the surface of the substrate. The morphological structure of the coating layer was determined through a Scanning Electron Microscope (SEM) examination utilizing the Phenom Pro X machine (Thermo Fisher Scientific, Waltham, MA, USA). The test results were subsequently analyzed using ImageJ software to quantify the porosity and unmelt materials.

The Olympus U-MSSP4 model (Evident Corporation, Tokyo, Japan) was used to perform Light Optical Microscope (LOM) tests to acquire an image of the coating layer. The obtained findings from this test were subsequently analyzed using ImageJ software to ascertain the thickness of the resultant coating layer. The Mitutoyo HM-21 (Mitutoyo Corporation, Kanagawa, Japan) was used to test coating hardness, following the ASTM E384 standards [43]. The experiment was conducted with a 0.5 kgf force for 10 seconds. The study involved tests on surface roughness, hardness, thickness, and the percentage of porosity and unmelt material. These tests were repeated three times, and the average value was computed based on the results.

Subsequently, specimens exhibiting the best surface roughness, hardness, thickness, and percentages of porosity and unmelt material were subjected to adhesion and corrosion rate testing. Adhesion testing was conducted to assess the bonding strength of the coating. This involved attaching a 20 mm diameter dolly to the coating layer, allowing it to sit undisturbed for 24 hours, and then applying force to the dolly using the DeFelsko PosiTest AT-A Automatic Adhesion Tester (manufactured by DeFelsko Corporation, New York, United States) under ASTM D454 standards. The corrosion rate testing in this study was conducted according to the ASTM G102 standard utilizing the SUGA Salt Spray Test Instrument manufactured by Nihon Denkei Co., Ltd. in Tokyo, Japan.

3. Result and Discussion

Figure 2.
Surface roughness
before and after
sandblasting

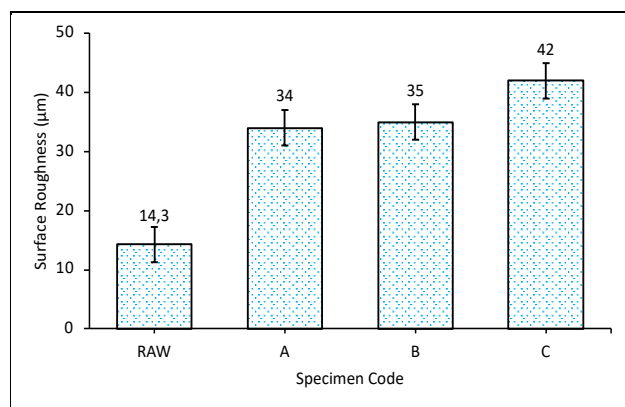


Figure 2 shows the results of measuring the substrate's surface roughness before and after sandblasting. The results of this investigation reveal that sandblasting increases the substrate's surface roughness. This can easily be observed in the RAW specimen, which has the lowest roughness compared to the other specimens. The levels of surface roughness for the RAW, A, B, and C specimens are 14.3 µm, 34 µm, 35 µm, and 42 µm, respectively.

Surface roughness increased with the number of sandblasting sessions. This phenomenon occurs due to the high-speed impact of abrasive particles, which causes erosion and removal of tiny particles from the surface of the substrate. Furthermore, the sandblasting procedure generates a profile of the new surface characterized by increased peaks and valleys. This leads to the creation of an irregular and rough surface [44], [45]. Papageorgiou et al.'s [45] research indicates that the sandblasting procedure, which employs a high-velocity particle stream propelled by compressed air, is effective for cleaning material surfaces. This is because sandblasting can remove undesirable oxides and contaminants. Furthermore, the sandblasting procedure has the capability to enhance surface energy, enhance adhesive surface area, and increase surface roughness. In addition, sandblasting is a technique for modifying the substrate surface and microstructure, where the main purpose of the sandblasting process is to make the surface texture of the substrate rougher so that it can improve the bonding of the substrate with the coating layer to be applied [37]. This study's findings align with Finger et al.'s [46] investigation. Their findings revealed that the sandblasting technique often enhances surface roughness. Furthermore, their research showed that blasting pressure, among the variables of blasting angle, working distance, and blasting pressure, had the most significant impact on surface roughness and residual stress on the substrate surface [46]. Additionally, a study by Iqbal et al. [47] shows that increasing the sandblasting process time from 2, 6, 10, 16, to 22 minutes makes the surface roughness of AISI 316L stainless steel much higher, from 0.67 µm to 1.46 µm.

SEM testing was conducted to determine the morphology of the coating structure. **Figure 3a–Figure 3c** depict the SEM test results for specimens A, B, and C at a magnification of 500x. The scanning electron microscopy (SEM) pictures of specimens A, B, and C reveal the existence of porosity, unmelted material, and oxides. The percentage of porosity and unmelted material was determined in this investigation using ImageJ software (**Figure 3d–Figure 3f**).

Figure 4 illustrates the impact of sandblasting repetition on the percentage of porosity and the amount of unmelted material. This study shows that repeating the sandblasting procedure 1–3 times increases the occurrence of porosity and unmelted material. The results of this investigation indicate that subjecting specimen C to the sandblasting procedure three times resulted in the highest percentage of porosity and unmelted material, which amounts to 13.794%. On the other hand, specimen A had the lowest percentage of porosity and unmelted material (7.122%) after repeating the sandblasting operation once.

The results of porosity and unmelted material in the specimens showed increasing results with specimens A, B and C of 7.122%, 9.784% and 13.794%, respectively. Based on A Teo et al. sandblasting can affect porosity and unmelt depending on several conditions such as pressure, time, abrasive particle size and material [48]. The significant increases in the percentage of porosity and unmelted material in this investigation can be ascribed to the enhancement in surface roughness induced by the sandblasting procedure. **Figure 5** depicts the relationship between the percentage of porosity and unmelted material to surface roughness of the substrate. This investigation discovered a positive correlation between the roughness of the substrate surface and the percentage of porosity and unmelted material in the coating layer. In other words, as the substrate surface becomes rougher, the percentage of porosity and unmelted material increases, and vice versa. Specimen A exhibits minimal surface roughness, producing the lowest porosity and unmelted material percentage. Conversely, specimen C, which had the highest surface roughness, exhibited the highest porosity and unmelted material percentage. This is due to the increasing

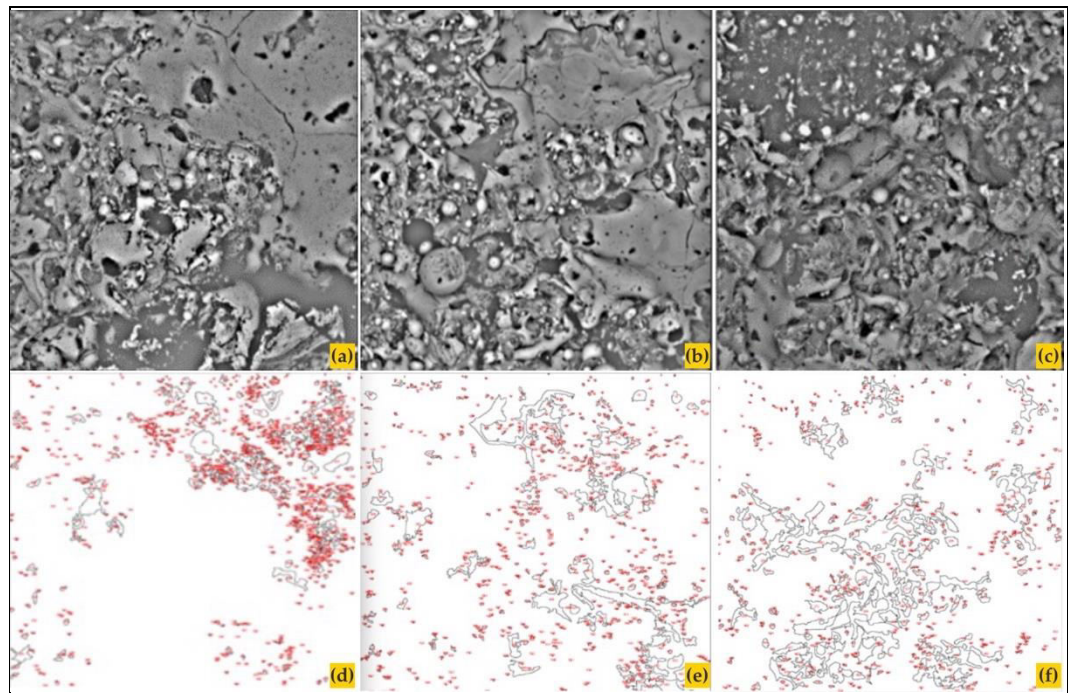


Figure 3. SEM images of specimens (a) A, (b) B, & (c) C and the calculation of porosity and unmelted material with ImageJ Software on specimens (d) A, (e) B, & (f) C

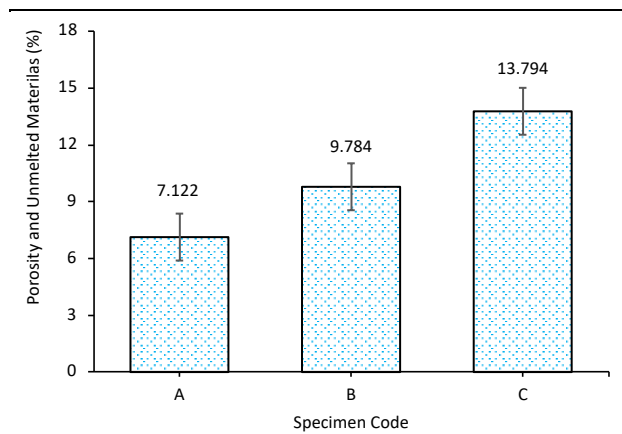


Figure 4. The influence of sandblasting process repetition on the percentage of porosity and unmelted material

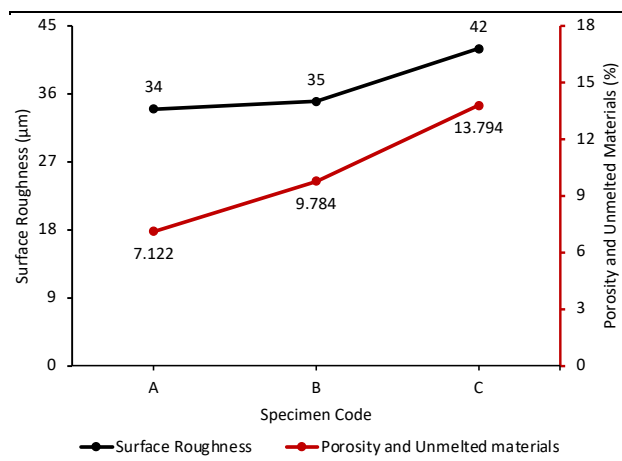


Figure 5. Effect of surface roughness on percentage of porosity and unmelted materials

surface roughness, the gaps in the coating tend to be close together, as a result many particles do not melt and create porosity cavities [49]. This study's findings are in line with the findings of Odhiambo et al. Their study demonstrated that the capacity to liquefy the coating material during the coating process diminished as the surface roughness of the substrate material increased. This can increase the amount of unmelted material and porosity [50]. According to Qiu et al.'s [51] research, the porosity of the specimen stays consistent when the average surface roughness (Ra) is less than 30 µm. Therefore, the porosity level in the sample increases when the average surface roughness (Ra) exceeds 30 µm [51]. Porosity has an influence on material characterization because it can be filled with water molecules, oxygen or other compounds that cause a decrease in corrosion resistance and decreased adhesion due to a less robust coating with the substrate [52].

The thickness of the resulting coating layer in this study is proven to

be influenced by sandblasting treatment repetition on the substrate surface, as illustrated in Figure 6. The thickness of the coating layer was obtained through calculations using ImageJ software on images obtained from microscope testing results. The findings in this study indicate that the thickness of the coating layer on specimens A, B, and C is 0.125 mm, 0.176 mm, and 0.249 mm, respectively. This demonstrates that the more sandblasting repetitions, the thicker the coating layer. Sandblasting is a surface treatment method that aims to clean and make the substrate surface rougher so that when given a coating, the coating material can stick well [38]. The findings of this investigation are consistent with the research carried out by Fernandez-Hernan et al. [53].

Their research demonstrated that AZ31 samples exhibited reduced roughness values when subjected to grit sheets with smaller grain sizes. Coating layers become thicker on substrate surfaces with greater roughness levels. This is because a surface with more roughness offers a more significant amount of space for the coating material to stick to, leading to a thicker coating. Moreover, substrates exhibiting greater roughness possess more profound grooves, which offer additional attachment sites for the coating material and enhance its overall thickness. According to studies conducted by Choudhary et al. [54], the reason for the rise in the thickness of the oxide layer on rough substrate surfaces is the presence of greater localized current densities. Consequently, the presence of an electric field enhances the dissolution of oxides, creating a thicker and more porous coating layer structure.

The study findings demonstrated a positive correlation between the number of sandblasting repeats and the thickness of the coating. The coating thickness is significantly influenced by the percentage of unmelted material and porosity (Figure 7). The results of this study demonstrate that the specimen with the most significant percentage of porosity and unmelted material had the thickest coating layer [54]. Conversely, the specimen with the smallest percentage of porosity and unmelted material exhibited the thinnest coating layer. A thinner coating layer is produced by stronger interlamellar bonding caused by a decrease in the percentage of porosity and unmelted material [5], [35], [36].

This is in line with the research of A Khokhlov et al using the microarc oxidation method, the more the thickness of the oxide layer increases, the porosity also increases because many cells are formed in the layer [55]. According to the research conducted by Manjunatha et al. [56], there is a clear correlation between the thickness of the coating layer and the rise in porosity within that layer. The coating layer becomes thicker as the porosity increases.

Figure 8 demonstrates the influence of repeated sandblasting treatment on the hardness of the coating layer. The hardness of the RAW, A, B, and C specimens were 206.8 HV, 1081.6 HV, 1009.4 HV, and 934 HV, respectively. Applying coatings using the TWAS approach enhanced the hardness of the substrate material. The substrate material's hardness (RAW specimen) was 206.8 HV and experienced a significant increase of 351% to 423% after applying the coating. The findings of this investigation indicate a direct correlation between the number of sandblasting repetitions and the extent of hardness reduction. This is evident in specimen C, which exhibits the lowest hardness compared to the other examples. The specimen with the highest hardness was specimen A, which underwent sandblasting treatment with one repeat.

Figure 6.
Thickness coating testing results

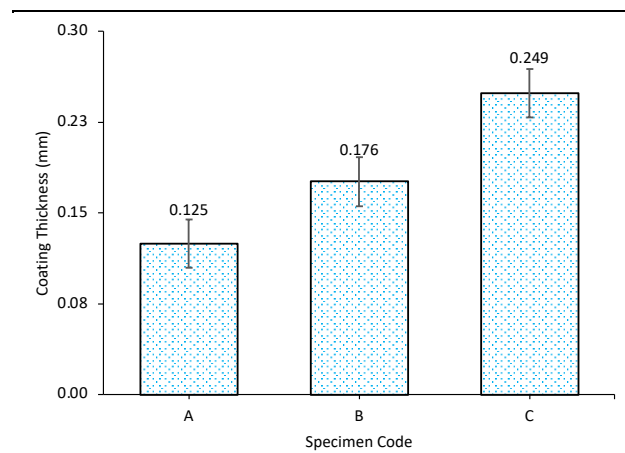


Figure 7.
Effect of porosity and unmelted materials (%) on coating thickness

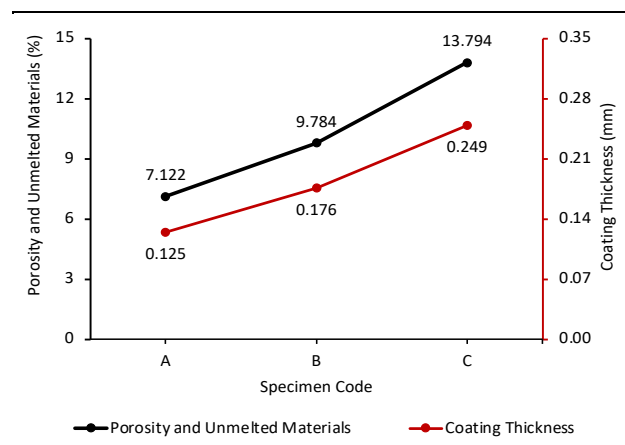
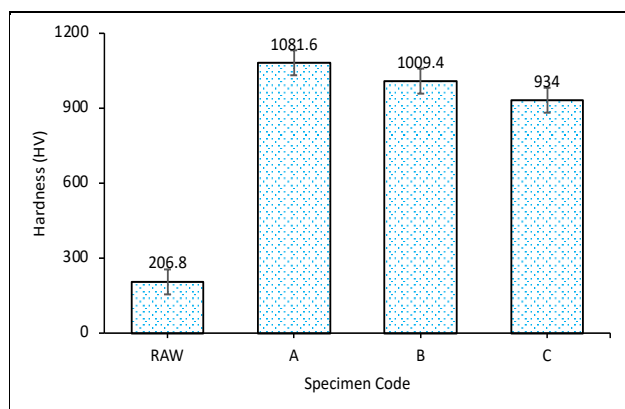


Figure 8.
Hardness of the specimens

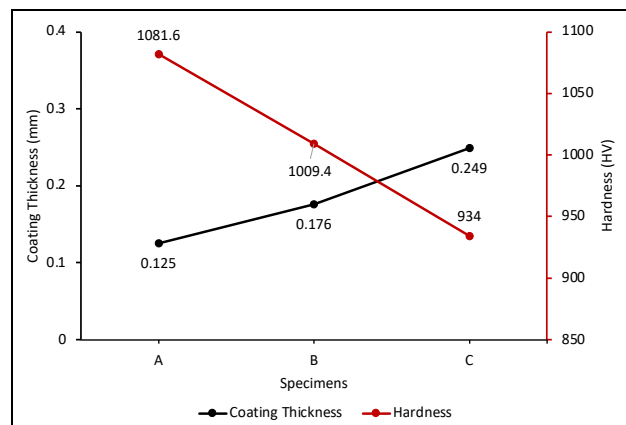


According to the results of this study, the substrate specimen with the slightest roughness had the most excellent coating hardness. This phenomenon arises due to a decrease in the roughness of the substrate surface, resulting in a reduction in the thickness and percentage of porosity and unmelted material formed in the coating layer. Consequently, there is an improvement in the hardness of the coating. The findings of this investigation are consistent with those of Gerald et al. [57]. Their investigation revealed the microhardness values of 1763HV, 1497HV, and 158.HV were obtained in the 650A, 550A, and substrate specimens. As the spraying current increases, the microhardness value also increases, resulting in a more compact coating layer with reduced porosity. According to Palanisamy et al. [58], reducing the amount of porosity can enhance the coating's microstructure and microhardness. The study conducted by Irawan et al. [5], also confirmed that the hardness of the coating increases as the percentage of porosity and unmelted material decreases. Porosity and unmelted material can negatively impact the cohesion of the coating, making it less capable of withstanding indentation loads and ultimately leading to a decrease in hardness. According to Tillman et al., this can occur due to non-uniform particle distribution causing porosity holes in the coating, so that the higher the porosity and unmelt, the lower the coating hardness is obtained [59].

In addition to the percentage of porosity and unmelted material, the thickness of the coating layer also significantly affects the hardness of the coating layer. The thicker the coating layer, the lower the hardness and vice versa (Figure 9). The study conducted by Manjunatha et al. [56] established a direct correlation between the thickness of the coating (measured in micrometres) and the microhardness of the coating (measured in HV). The reduction in microhardness as the

thickness of plasma-sprayed molybdenum (Mo) coatings increases can be attributed to the greater quantity of trapped gas and thermal shrinkage in thicker coatings. The greater porosity increases the number of empty spaces inside the material, decreasing its hardness. Moreover, thicker layers have elevated stress concentrations. This can result in cracks, delamination, and fractures on the coating's surface. These flaws additionally contribute to the decrease in microhardness.

Figure 9.
The relationship between coating thickness and hardness of the specimens



Regarding the specimens examined in this study, Specimen A exhibited the lowest surface roughness on the substrate. Consequently, it displayed the lowest percentage of porosity and unmelted material compared to the other specimens. This results in the creation of the thinnest possible coating layer and the maximum hardness level in the coating layer. As the coating layer's hardness increases, the wear rate decreases, and the wear resistance improves [60]. The findings of this investigation are consistent with the research carried out by Zhao et al. [61]. Their research findings indicate an inverse relationship between the increase in hardness of Ti-Al-Si coatings and the wear rate. Enhancing the hardness of the Ti-Al-Si coatings layer results in a reduction in the rate of wear. The wear rates ($\times 10^{-16} \text{ m}^3/\text{Nm}$) of the specimens with hardnesses of 740 HV, 704 HV, and 680 HV were 3.68, 3.9, and 4.89, respectively. According to Xie et al.'s [62] research, an increase in the weight percentage of WC leads to a corresponding increase in the hardness value of Co-based composite coatings. The Co-based composite coating hardness was 553.43, 577.25, 782.45, 801.59, and 954.64 following the addition of WC at 0%, 10%, 20%, 30%, and 40%, respectively. Furthermore, the increased hardness correspondingly led to reduced weight loss during wear tests. The weight loss of the Co-based composite coating decreased as the percentage of WC addition increased. Furthermore, the weight loss values for WC additions of 0%, 10%, 20%, 30%, and 40% were 1.12, 1, 0.5, 0.37, and 0.33, respectively. As weight loss decreases, wear resistance increases.

In this study, specimen A was the sole subject of the coating adhesion and corrosion rate tests. This was done due to the superior properties achieved in specimen A compared to the other specimens. The adhesion strength of the coating layer on specimen A measured 14.5 MPa. In general, coating adhesion describes the connection that exists between the substrate and the coating layer. The force necessary to separate the coating layer from the substrate is used to determine coating adhesion [63]. According to studies by Michael Pfeifer [64], the adhesion of

coatings is influenced by the condition of the substrate's surface. The adhesion of the coating can be compromised by oxidation on the substrate surface. Poor adhesion can result from contamination of the substrate surface, such as dirt or oil. The substrate's surface texture is significant for coating adherence because it influences the mechanical bond between the coating material and the substrate. Typically, the substrate is roughened to facilitate the adhesion of the coating material to the substrate surface. The adhesion of the coating layer created in this study was 14.5 MPa, which fulfilled the criterion for adhesion of the coating layer formed using the TWAS method (10-40 MPa) [5]. The coating layer generated in this study exhibits a higher level of adhesion than that of the studies performed by Ismail et al. [65] and Purniawan et al. [66]. Adhesion of the wire arc sprayed Al-Zn pseudo-alloy coating layer is between 6.1 and 8.34 MPa [65]. The adhesion level of the coated layer in Purniawan et al.'s investigation ranges from 9.93 to 11.72 MPa [66].

Figure 10.
Corrosion rate
testing result on
specimens

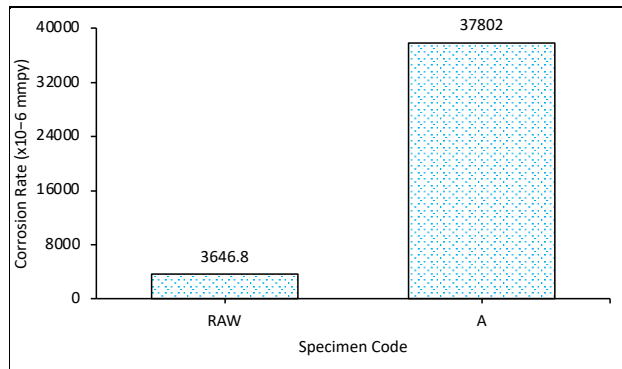


Figure 10 compares the corrosion rates of RAW and A specimens. The investigation reveals that the corrosion rate (x10⁻⁶ mmpy) of RAW and A specimens is 3648.6 and 37,802, respectively. The study's findings indicate that the corrosion rate of the substrate material is comparatively lower than specimen A's. This suggests that the substrate material has a higher corrosion resistance level than specimen A.

The findings of this investigation suggest that exposing the substrate material to sandblasting treatment leads to a reduction in its corrosion resistance. This finding aligns with the study performed by Geng et al. [67]. According to their research, sandblasting significantly reduced the corrosion resistance of 316L stainless steel. This was attributed to changes in the surface structure, the creation of the α' -martensite phase, and increased dislocation density. Resistance to corrosion is the capacity to protect a substrate from corrosion. The existence of open porosity and cracks has a stronger effect on corrosion resistance than the chemical composition of a coating material [68]. The process of material degradation can be accelerated by the presence of corrosive substances in the coating layer, which can enter through porosity and unmelted material. Coatings are typically applied to the surface of materials to enhance their resistance to abrasion, wear, corrosion, and various environmental factors. Nevertheless, the protective properties of coatings may be compromised by the presence of unmelted material and porosity. There are numerous factors that can contribute to the formation of unmelted material and porosity in coating layers, such as the surface preparation, coating process, and the material's composition. The findings of this analysis indicate that the porosity and unmelted material in specimen A amount to 7.122%. The existence of porosity and unmelted material inside the coating layer results in inadequate adhesion of the coating layer and facilitates elevated rates of corrosion [69]. Furthermore, the existence of porosity in the coating layer serves as a pathway for corrosive substances to infiltrate the contact between the coating and the substrate. This can expedite the process of rusting [70]. The potentiodynamic polarization tests by García-Cabezón et al. [71] revealed that the porous samples lacked a stable passive plain and demonstrated greater corrosion current values than the solid samples. Furthermore, the porous samples exhibited a less durable oxide layer, resulting in diminished protective characteristics. The infiltration of the electrolyte into the pores causes the formation of a less effective oxide layer, leading to localized corrosion.

Li et al. [72] conducted research indicating that Fe-based amorphous composite coatings exhibit stronger corrosion resistance since they have lower porosity and higher amorphous content. Nevertheless, since the amount of amorphous content is minimal, the porosity level is the primary aspect influencing corrosion resistance in the coating. Yoo et al. discovered that the coating with an amorphous structure had greater resistance to corrosion compared to the coating with a crystallized structure. Nevertheless, the application of heat treatment following to the coating procedure resulted in a reduction in corrosion resistance [73].

4. Conclusion

This study investigated the influence of repeating the sandblasting treatment on the surface roughness of the substrate and the characteristics of the resultant coating layer. This study examined the porosity and unmelted material percentage, thickness, hardness, adhesion strength, and corrosion resistance of coating layers under different sandblasting treatment repetitions. The study findings demonstrate that the application of sandblasting treatment substantially enhances the surface roughness of the 304 stainless steel substrates. The roughness measurements for the RAW, A, B, and C specimens were 14.3 μm , 34 μm , 35 μm , and 42 μm , respectively. The rise in roughness is closely correlated with the number of sandblasting repetitions. Surface roughness and the percentage of porosity and unmelted material in the coating layer exhibit a positive correlation, as indicated by the results of this study. The substrate material's surface roughness increases as sandblasting repetitions increase. This leads to an increase in the percentage of unmelted material and porosity in the coating layer. The porosity and unmelted material percentages in specimens A, B, and C are 7.122%, 9.784%, and 13.794%, respectively. An increase in the percentage of porosity and unmelted material increases the thickness and decreases the hardness of the resultant coating layer. The coating layer thickness in examples A, B, and C is 0.125 mm, 0.176 mm, and 0.249 mm, respectively. The specimens A, B, and C have hardness values of 1081.6 HV, 1009.4 HV, and 934 HV, respectively. The TWAS coating process employed in this investigation demonstrated its efficacy in enhancing the hardness of the substrate material. The substrate material (RAW specimen) had a hardness of 206.8 HV and underwent a substantial increase of 351% to 423% after being coated. The adhesion of the coating layer produced in this study was measured to be 14.5 MPa, which satisfies the adhesion requirements for coating layers made using the TWAS method. The study's findings indicate that the corrosion rate of the substrate material is comparatively lower than specimen A. The corrosion rate ($\times 10^{-6}$ mmpy) for the RAW specimen is 3648.6, while for the A specimen it is 37,802. Exposing the substrate material to sandblasting treatment results in a reduction in its corrosion resistance. Porosity in the coating layer facilitates the infiltration of corrosive chemicals into the interface between the coating and the substrate. This can expedite the rusting process.

Acknowledgments

The author would like to express their gratitude to Universitas Negeri Semarang for supporting this research and Universitas Tarumanagara for giving funding through the Research International Collaboration Grant No: 011-Int-BGRA-I-KLPPM/UNTAR/XII/2022.

Authors' Declaration

Authors' contributions and responsibilities - The authors made substantial contributions to the conception and design of the study. The authors took responsibility for data analysis, interpretation, and discussion of results. The authors read and approved the final manuscript.

Funding – has been explained in the Acknowledgments.

Availability of data and materials - All data is available from the authors.

Competing interests - The authors declare no competing interest.

Additional information – No additional information from the authors.

References

- [1] Y. Li, H. Su, Y. Wang, W. Jiang, and Q. Zhu, "Dynamic Characteristic Analysis of Centrifugal Pump Impeller Based on Fluid-Solid Coupling," *Journal of Marine Science and Engineering*, vol. 10, no. 7, p. 880, Jun. 2022, doi: 10.3390/jmse10070880.
- [2] A. Nasir, E. Dribssa, and M. Girma, "The pump as a turbine: A review on performance prediction, performance improvement, and economic analysis," *Heliyon*, vol. 10, no. 4, p. e26084, Feb. 2024, doi: 10.1016/j.heliyon.2024.e26084.
- [3] G. J. P. and M. D. L. William C. Lyons, "Auxiliary Equipment," in *Standard Handbook of Petroleum and Natural Gas Engineering*, W. C. Lyons, G. J. Plisga, and M. D. B. T.-S. H. of P. and N. G. E. (Third E. Lorenz, Eds. Boston: Elsevier, 2016, pp. 3-1-3–66.

- [4] P. Koukouvinis, M. Murali-Girija, I. K. Karathanassis, and M. Gavaises, "Cavitation in Positive Displacement Pumps," in *Cavitation and Bubble Dynamics*, P. Koukouvinis and M. B. T.-C. and B. D. Gavaises, Eds. Elsevier, 2021, pp. 303–329.
- [5] A. P. Irawan et al., "Influence of Post-Heat Treatment on the Characteristics of FeCrBMnSi Coating on Stainless Steel 304 Substrate Prepared by Twin Wire Arc Spray (TWAS) Method at Various Stand-off Distance," *Jordan Journal of Mechanical and Industrial Engineering*, vol. 18, no. 02, pp. 327–337, May 2024, doi: 10.59038/jjmie/180206.
- [6] R. Ramakrishna, S. Hemalatha, and D. S. Rao, "Analysis and performance of centrifugal pump impeller," *Materials Today: Proceedings*, vol. 50, pp. 2467–2473, 2022, doi: 10.1016/j.matpr.2021.10.364.
- [7] N. Pokharel, A. Ghimire, B. Thapa, and B. S. Thapa, "Wear in centrifugal pumps with causes, effects and remedies: A Review," *IOP Conference Series: Earth and Environmental Science*, vol. 1037, no. 1, p. 012042, Jun. 2022, doi: 10.1088/1755-1315/1037/1/012042.
- [8] G. Peng, Q. Chen, L. Bai, Z. Hu, L. Zhou, and X. Huang, "Wear mechanism investigation in a centrifugal slurry pump impeller by numerical simulation and experiments," *Engineering Failure Analysis*, vol. 128, no. 105637, p. 105637, Oct. 2021, doi: 10.1016/j.engfailanal.2021.105637.
- [9] R. O. P. Serrano, L. P. Santos, E. M. de F. Viana, M. A. Pinto, and C. B. Martinez, "Case study: Effects of sediment concentration on the wear of fluvial water pump impellers on Brazil's Acre River," *Wear*, vol. 408–409, pp. 131–137, Aug. 2018, doi: 10.1016/j.wear.2018.04.018.
- [10] G. Peng, F. Fan, L. Zhou, X. Huang, and J. Ma, "Optimal hydraulic design to minimize erosive wear in a centrifugal slurry pump impeller," *Engineering Failure Analysis*, vol. 120, no. 105105, p. 105105, Feb. 2021, doi: 10.1016/j.engfailanal.2020.105105.
- [11] C. Kang, Q. Cao, S. Teng, H. Liu, and K. Ding, "Wear characteristics of a centrifugal pump transporting solid–liquid mixture: An experimental and numerical study," *Ain Shams Engineering Journal*, vol. 15, no. 1, p. 102277, Jan. 2024, doi: 10.1016/j.asej.2023.102277.
- [12] A. Goswami, S. C. Pillai, and G. McGranaghan, "Micro/Nanoscale surface modifications to combat heat exchanger fouling," *Chemical Engineering Journal Advances*, vol. 16, p. 100519, Nov. 2023, doi: 10.1016/j.ceja.2023.100519.
- [13] L. A. Dobrzański and J. Madejski, "Prototype of an expert system for selection of coatings for metals," *Journal of Materials Processing Technology*, vol. 175, no. 1–3, pp. 163–172, Jun. 2006, doi: 10.1016/j.jmatprotec.2005.04.034.
- [14] K. K. Amirtharaj Mosas, A. R. Chandrasekar, A. Dasan, A. Pakseresht, and D. Galusek, "Recent Advancements in Materials and Coatings for Biomedical Implants," *Gels*, vol. 8, no. 5, p. 323, May 2022, doi: 10.3390/gels8050323.
- [15] S. Junus et al., "Effect of current, time, ethanol concentration, and pH electrolyte on ZnO coated carbon fiber using electrochemical deposition method," *Mechanical Engineering for Society and Industry*, vol. 3, no. 2, pp. 105–113, 2023, doi: 10.31603/mesi.10493.
- [16] Y. Subagyo et al., "Development of magnesium biocomposites with hydroxyapatite or carbonate apatite reinforcement as implant candidates: A review," *Mechanical Engineering for Society and Industry*, vol. 3, no. 3, pp. 152–165, 2023, doi: 10.31603/mesi.10389.
- [17] J. Andrean, A. Harmayanti, A. Wahjudi, and A. Syamlan, "Analysis of The Corrosion Inhibition Efficacy of Camellia Sinensis Extract on Aluminium 6061 Alloys using Artificial Neural Network (ANN)," *Mechanics Exploration and Material Innovation*, vol. 1, no. 2, pp. 67–74, Apr. 2024, doi: 10.21776/ub.memi.2024.001.02.5.
- [18] S. Saifudin, W. Purwanto, and J. C. T. Su, "Characteristics of Diamond-Like Carbon Coating Using Plasma Assisted Chemical Vapor Deposition on Steel Tool," *Automotive Experiences*, vol. 3, no. 1, pp. 27–32, Apr. 2020, doi: 10.31603/ae.v3i1.3417.
- [19] A. D. Shieddieque, I. Rahayu, S. Hidayat, and J. A. Laksmono, "Recent Development in LiFePO4 Surface Modifications with Carbon Coating from Originated Metal-Organic Frameworks (MOFs) to Improve the Conductivity of Cathode for Lithium-Ion Batteries: A Review and Bibliometrics Analysis," *Automotive Experiences*, vol. 6, no. 3, pp. 438–451, Nov. 2023, doi: 10.31603/ae.9524.
- [20] T. Raja, M. Setiyo, V. Murugan, and S. Dhandapani, "Analysis of the Temperature Variation of Bizarre Thermal Barrier Coatings and their impacts on Engine," *Automotive Experiences*, vol. 6, no. 3, pp. 497–514, Nov. 2023, doi: 10.31603/ae.9802.

- [21] S. N. S. Z. Abidin, W. H. Azmi, N. N. M. Zawawi, and A. I. Ramadhan, "Comprehensive Review of Nanoparticles Dispersion Technology for Automotive Surfaces," *Automotive Experiences*, vol. 5, no. 3, pp. 304–327, Jun. 2022, doi: 10.31603/ae.6882.
- [22] G. Singh, "A review on erosion wear of different types of slurry pump impeller materials," *Materials Today: Proceedings*, vol. 37, no. Part 2, pp. 2298–2301, 2021, doi: 10.1016/j.matpr.2020.07.727.
- [23] Z. Ruizhu, L. Jingrui, Y. Dakao, and Z. Yuanyuan, "Mechanical Properties of WC-8Co Wear-Resistant Coating on Pump Impellers Surface by Electro-Spark," *Rare Metal Materials and Engineering*, vol. 44, no. 7, pp. 1587–1590, Jul. 2015, doi: 10.1016/S1875-5372(15)30097-7.
- [24] D. Lee, S. Krumdieck, and S. D. Talwar, "Scale-up design for industrial development of a PP-MOCVD coating system," *Surface and Coatings Technology*, vol. 230, pp. 39–45, Sep. 2013, doi: 10.1016/j.surfcoat.2013.06.064.
- [25] Y. Wang et al., "Slurry erosion–corrosion behaviour of high-velocity oxy-fuel (HVOF) sprayed Fe-based amorphous metallic coatings for marine pump in sand-containing NaCl solutions," *Corrosion Science*, vol. 53, no. 10, pp. 3177–3185, Oct. 2011, doi: 10.1016/j.corsci.2011.05.062.
- [26] P. Smith and T. Kraenzler, "Reducing effects of corrosion and erosion," *World Pumps*, vol. 2017, no. 2, pp. 38–41, Feb. 2017, doi: 10.1016/S0262-1762(17)30033-0.
- [27] P. A. Deshmukh, K. D. Deshmukh, and N. A. Mandhare, "Performance enhancement of centrifugal pump by minimizing casing losses using coating," *SN Applied Sciences*, vol. 2, no. 2, p. 252, Feb. 2020, doi: 10.1007/s42452-020-2042-7.
- [28] C. Liu, H. Lu, E. Qin, L. Ye, and S. Wu, "The FeCr-Based Coating by On-Site Twin-Wire Arc Spraying for Proactive Maintenance of Power Plant Components," *Journal of Thermal Spray Technology*, vol. 30, no. 4, pp. 959–967, Apr. 2021, doi: 10.1007/s11666-020-01138-y.
- [29] K. DePalma, M. Walluk, L. P. Martin, and K. Sisak, "Investigation of Mechanical Properties of Twin Wire Arc Repair of Cast Iron Components," *Journal of Thermal Spray Technology*, vol. 31, no. 1–2, pp. 315–328, Jan. 2022, doi: 10.1007/s11666-021-01304-w.
- [30] Š. Houdková, P. Šulcová, K. Lencová, Z. Česánek, and M. Švantner, "Twin Wire Arc Sprayed Coatings for Power Industry Applications – process parameters optimization study," *Journal of Physics: Conference Series*, vol. 2572, no. 1, p. 012001, Aug. 2023, doi: 10.1088/1742-6596/2572/1/012001.
- [31] L. Govind Sanjeev Kumar, D. Thirumalaikumarasamy, K. Karthikeyan, M. Mathanbabu, and T. Sonar, "Optimization of process parameters for minimizing porosity level and maximizing hardness of AA2024 alloy coating on AZ31B alloy using computational response surface methodology," *International Journal on Interactive Design and Manufacturing (IJIDeM)*, pp. 1–15, Sep. 2023, doi: 10.1007/s12008-023-01501-7.
- [32] J. Bang and E. Lee, "Evaluation of the Mechanical and Corrosion Behavior of Twin Wire Arc Sprayed Ni-Al Coatings with Different Al and Mo Content," *Coatings*, vol. 13, no. 6, p. 1069, Jun. 2023, doi: 10.3390/coatings13061069.
- [33] N. Wagner, "Effect of Process Parameters on Twin Wire Arc Sprayed Steel Coatings," *Journal of Materials Engineering and Performance*, vol. 30, no. 9, pp. 6650–6655, Sep. 2021, doi: 10.1007/s11665-021-05941-8.
- [34] H. Liu et al., "Direct deposition of low-cost carbon fiber reinforced stainless steel composites by twin-wire arc spray," *Journal of Materials Processing Technology*, vol. 301, p. 117440, Mar. 2022, doi: 10.1016/j.jmatprotec.2021.117440.
- [35] D. F. Fitriyana et al., "The Effect of Compressed Air Pressure and Stand-off Distance on the Twin Wire Arc Spray (TWAS) Coating for Pump Impeller from AISI 304 Stainless Steel," *Springer Proceedings in Physics*, vol. 242, pp. 119–130, 2020, doi: 10.1007/978-981-15-2294-9_11.
- [36] D. F. Fitriyana et al., "The Effect of Post-Heat Treatment on The Mechanical Properties of FeCrBMnSi Coatings Prepared by Twin Wire Arc Spraying (TWAS) Method on Pump Impeller From 304 Stainless Steel," *Journal of Advanced Research in Fluid Mechanics and Thermal Sciences*, vol. 2, no. 2, pp. 138–147, 2022, doi: 10.37934/arfmts.93.2.138147.
- [37] H.-Y. Wang et al., "Effect of sandblasting intensity on microstructures and properties of pure titanium micro-arc oxidation coatings in an optimized composite technique," *Applied Surface Science*, vol. 292, pp. 204–212, Feb. 2014, doi: 10.1016/j.apsusc.2013.11.115.

- [38] A. Rudawska, I. Danczak, M. Müller, and P. Valasek, "The effect of sandblasting on surface properties for adhesion," *International Journal of Adhesion and Adhesives*, vol. 70, pp. 176–190, Oct. 2016, doi: 10.1016/j.ijadhadh.2016.06.010.
- [39] N. Hammouda and K. Belmokre, "Effect of surface treatment by sandblasting on the quality and electrochemical corrosion properties of a C-1020 carbon steel used by an Algerian oil company," *MATEC Web of Conferences*, vol. 272, p. 01001, Mar. 2019, doi: 10.1051/matecconf/201927201001.
- [40] Thyssenkrupp Materials Company, "AISI 304 Stainless steel data sheet," 2018.
- [41] Praxair and Tafa Technologies, "Praxair and Tafa Arc Spray BondArc® Wire75B® Back to Wire Catalog," 2020.
- [42] M. Review and A. Review, "Praxair and Tafa 95MXC® UltraHard® Wire Coating Physical Properties," 2020.
- [43] T. S. Amosun, S. O. Hammed, A. M. G. De Lima, and I. Habibi, "Effect of quenching media on mechanical properties of welded mild steel plate," *Mechanical Engineering for Society and Industry*, vol. 3, no. 1, pp. 4–11, Sep. 2022, doi: 10.31603/mesi.7121.
- [44] M. Kaladhar, K. Venkata Subbaiah, and C. H. Srinivasa Rao, "Optimization of surface roughness and tool flank wear in turning of AISI 304 austenitic stainless steel with CVD coated tool," *Journal of Engineering Science and Technology*, vol. 8, no. 2, pp. 165–176, 2013.
- [45] S. N. Papageorgiou and N. Pandis, "Clinical evidence on orthodontic bond failure and associated factors," in *Orthodontic Applications of Biomaterials*, T. Eliades and W. A. B. T.-O. A. of B. Brantley, Eds. Elsevier, 2017, pp. 191–206.
- [46] C. Finger, M. Stiesch, M. Eisenburger, B. Breidenstein, S. Busemann, and A. Greuling, "Effect of sandblasting on the surface roughness and residual stress of 3Y-TZP (zirconia)," *SN Applied Sciences*, vol. 2, no. 10, p. 1700, Oct. 2020, doi: 10.1007/s42452-020-03492-6.
- [47] M. Iqbal et al., "The effect of sandblasting on AISI 316L stainless steels," in *Prosiding Industrial Research Workshop and National Seminar*, 2011, pp. 58–61.
- [48] A. Q. A. Teo, L. Yan, A. Chaudhari, and G. K. O'Neill, "Post-Processing and Surface Characterization of Additively Manufactured Stainless Steel 316L Lattice: Implications for BioMedical Use," *Materials*, vol. 14, no. 6, p. 1376, Mar. 2021, doi: 10.3390/ma14061376.
- [49] D. Tejero-Martin, M. Bai, J. Mata, and T. Hussain, "Evolution of porosity in suspension thermal sprayed YSZ thermal barrier coatings through neutron scattering and image analysis techniques," *Journal of the European Ceramic Society*, vol. 41, no. 12, pp. 6035–6048, Sep. 2021, doi: 10.1016/j.jeurceramsoc.2021.04.020.
- [50] J. G. Odhiambo, W. Li, Y. Zhao, and C. Li, "Porosity and Its Significance in Plasma-Sprayed Coatings," *Coatings*, vol. 9, no. 7, p. 460, Jul. 2019, doi: 10.3390/coatings9070460.
- [51] C. Qiu, C. Panwisawas, M. Ward, H. C. Basoalto, J. W. Brooks, and M. M. Attallah, "On the role of melt flow into the surface structure and porosity development during selective laser melting," *Acta Materialia*, vol. 96, pp. 72–79, Sep. 2015, doi: 10.1016/j.actamat.2015.06.004.
- [52] N. Kazamer, R. Muntean, P. C. Vălean, D. T. Pascal, G. Mărginean, and V.-A. Șerban, "Comparison of Ni-Based Self-Fluxing Remelted Coatings for Wear and Corrosion Applications," *Materials*, vol. 14, no. 12, p. 3293, Jun. 2021, doi: 10.3390/ma14123293.
- [53] J. P. Fernández-Hernán, A. J. López, B. Torres, and J. Rams, "Influence of roughness and grinding direction on the thickness and adhesion of sol-gel coatings deposited by dip-coating on AZ31 magnesium substrates. A Landau–Levich equation revision," *Surface and Coatings Technology*, vol. 408, p. 126798, Feb. 2021, doi: 10.1016/j.surfcoat.2020.126798.
- [54] R. K. Choudhary, K. P. Sreeshma, and P. Mishra, "Effect of Surface Roughness of an Electropolished Aluminum Substrate on the Thickness, Morphology, and Hardness of Aluminum Oxide Coatings Formed During Anodization in Oxalic Acid," *Journal of Materials Engineering and Performance*, vol. 26, no. 7, pp. 3614–3620, Jul. 2017, doi: 10.1007/s11665-017-2798-0.
- [55] A. Khokhlov, D. Maryin, D. Molochnikov, A. Khokhlov, I. Gayaziev, and O. Smirnova, "Influence of the thickness and porosity of the oxide coating on the piston heads depending on the parameters of the microarc oxidation mode," *Journal of Physics: Conference Series*, vol. 2131, no. 4, 2021, doi: 10.1088/1742-6596/2131/4/042046.
- [56] S. S. Manjunatha and S. Basavarajappa, "Effect of coating thickness on properties of Mo coatings deposited by plasma spraying," *Tribology - Materials, Surfaces and Interfaces*, vol. 9,

- no. 1, pp. 41–45, 2015, doi: 10.1179/1751584X14Y.0000000083.
- [57] O. J. Gerald, L. Wenge, Z. Yuan Tao, L. Cheng Long, and L. Qiang, “Influence of plasma spraying current on the microstructural characteristics and tribological behaviour of plasma sprayed Cr₂O₃ coating,” *Boletin de la Sociedad Espanola de Ceramica y Vidrio*, vol. 60, no. 6, pp. 338–346, 2021, doi: 10.1016/j.bsecv.2020.03.007.
- [58] K. Palanisamy, S. Gangolu, and J. Mangalam Antony, “Effects of HVOF spray parameters on porosity and hardness of 316L SS coated Mg AZ80 alloy,” *Surface and Coatings Technology*, vol. 448, pp. 1–13, 2022, doi: 10.1016/j.surfcoat.2022.128898.
- [59] W. Tillmann, O. Khalil, and M. Abdulgader, “Porosity Characterization and Its Effect on Thermal Properties of APS-Sprayed Alumina Coatings,” *Coatings*, vol. 9, no. 10, p. 601, Sep. 2019, doi: 10.3390/coatings9100601.
- [60] O. R. Adetunji, A. M. Adedayo, S. O. Ismailia, O. U. Dairo, I. K. Okediran, and O. M. Adesusi, “Effect of silica on the mechanical properties of palm kernel shell based automotive brake pad,” *Mechanical Engineering for Society and Industry*, vol. 2, no. 1, pp. 7–16, 2022, doi: 10.31603/mesi.6178.
- [61] T. Zhao *et al.*, “Enhancement in the Wear Resistance of Ti-Al-Si Coatings Fabricated by Hot Dipping,” *JOM*, vol. 76, no. 9, pp. 5048–5058, Sep. 2024, doi: 10.1007/s11837-024-06545-y.
- [62] Z. Xie *et al.*, “Microstructure and wear resistance of WC/Co-based coating on copper by plasma cladding,” *Journal of Materials Research and Technology*, vol. 15, pp. 821–833, 2021, doi: 10.1016/j.jmrt.2021.08.114.
- [63] R. S. R. Kalidindi and R. Subasri, “Sol-gel nanocomposite hard coatings,” in *Anti-Abrasive Nanocoatings*, M. B. T.-A.-A. N. Aliofkhazraei, Ed. Elsevier, 2015, pp. 105–136.
- [64] M. Pfeifer, “Manufacturing Process Considerations,” in *Materials Enabled Designs*, M. B. T.-M. E. D. Pfeifer, Ed. Boston: Elsevier, 2009, pp. 115–160.
- [65] N. S. Ismail, N. A. Fadil, and T. A. A. Bakar, “Effect of stand-off distance on the microstructural and mechanical properties of Al-Zn pseudo-alloy coating prepared via wire arc spray process,” *Malaysian Journal of Microscopy*, vol. 18, no. 1, pp. 256–269, 2022.
- [66] A. Purniawan, H. Irawan, and S. T. Wicaksono, “Microstructure and Adhesion Properties Post-Annealed Metallic Coating of FeCrBmnsi on Tube and Internal Structure Coal-Fired Boiler,” *IPTEK Journal of Proceedings Series*, vol. 0, no. 1, pp. 98–103, 2017, doi: 10.12962/j23546026.y2017i1.2200.
- [67] S. Geng, J. Sun, and L. Guo, “Effect of sandblasting and subsequent acid pickling and passivation on the microstructure and corrosion behavior of 316L stainless steel,” *Materials and Design*, vol. 88, pp. 1–7, 2015, doi: 10.1016/j.matdes.2015.08.113.
- [68] L.-M. Berger, “Coatings by Thermal Spray,” in *Comprehensive Hard Materials*, vol. 1, Elsevier, 2014, pp. 471–506.
- [69] A. K. Basak, P. Matteazzi, M. Vardavoulias, and J.-P. Celis, “Corrosion–wear behaviour of thermal sprayed nanostructured FeCu/WC–Co coatings,” *Wear*, vol. 261, no. 9, pp. 1042–1050, Nov. 2006, doi: 10.1016/j.wear.2006.03.026.
- [70] S. D. Zhang, J. Wu, W. B. Qi, and J. Q. Wang, “Effect of porosity defects on the long-term corrosion behaviour of Fe-based amorphous alloy coated mild steel,” *Corrosion Science*, vol. 110, pp. 57–70, Sep. 2016, doi: 10.1016/j.corsci.2016.04.021.
- [71] C. García-Cabezón, V. Godinho, C. Salvo-Comino, Y. Torres, and F. Martín-Pedrosa, “Improved corrosion behavior and biocompatibility of porous titanium samples coated with bioactive chitosan-based nanocomposites,” *Materials*, vol. 14, no. 21, pp. 1–20, 2021, doi: 10.3390/ma14216322.
- [72] C. Li, Y. Zhang, J. Zhai, C. Li, and S. Kou, “Effects of heat treatment on microstructure and properties of Fe-based amorphous composite coatings,” *Materials Science and Technology*, vol. 39, no. 15, pp. 2168–2178, Oct. 2023, doi: 10.1080/02670836.2023.2195750.
- [73] Y. H. Yoo, S. H. Lee, J. G. Kim, J. S. Kim, and C. Lee, “Effect of heat treatment on the corrosion resistance of Ni-based and Cu-based amorphous alloy coatings,” *Journal of Alloys and Compounds*, vol. 461, pp. 304–311, 2008, doi: 10.1016/j.jallcom.2007.06.118.